

Single-Grating Monolithic Spatial Heterodyne Raman Spectrometer—A Potential Tool for Planetary Exploration. E. M. Kelly¹, M. J. Egan¹, A. Colon², S. M. Angel², and S. K. Sharma², ¹ Hawaii Institute of Geophysics and Planetology, University of Hawaii at Manoa, Honolulu, Hawaii'i, ² Department of Chemistry and Biochemistry, University of South Carolina, Columbia, South Carolina. Correspondence email: evamk@hawaii.edu

Introduction: Advances in Raman instrumentation have led to the implementation of a remote dispersive Raman spectrometer on the Perseverance rover on Mars, which is used for remote sensing. [1] For remote applications, dispersive spectrometers suffer from a few setbacks such as relatively larger sizes, low light throughput, limited spectral ranges, and relatively low resolutions for small devices, and high sensitivity to misalignment. A spatial heterodyne Raman spectrometer (SHRS), which is a fixed grating interferometer, helps overcome some of these problems. Most SHRS devices that have been described use two fixed diffraction gratings, but a variance of the SHRS called the one-grating SHRS (1g-SHRS) replaces one of the gratings with a mirror, which makes it more compact. [2] In a recent paper, we described monolithic 2-gratings SHRS [3], and in this paper, we investigate a single-grating monolithic SHRS (1g-mSHRS), which combines the 1g-SHRS with a monolithic setup previously tested at the University of South Carolina.

Experimental: To test the 1g-mSHRS device, spectra were collected using a 532 nm pulsed Nd:YAG laser to illuminate a liquid/solid sample. A telescope then collected the scattered light and directed it into the monolith, where the light was recombined. The recombined light was then sent through a collecting lens to an intensity charged-coupled device (ICCD) camera, and is displayed in Figure 1. The data collected with mm-SHRS on powered samples of KClO_3 , NH_4NO_3 , sulfur and minerals dolomite, calcite, gypsum, barite, quartz; and organic liquids C_6H_{12} , CH_3OH , C_{10}H_8 , and CH_3CN , and solid naphthalene (C_{10}H_8) were then processed using a Fast Fourier transform. This configuration was however in the 1D conformation (as opposed to the 2D configuration – see results & discussion) which combined with the Littrow wavelength being positioned at 595 nm resulted in an aliasing effect, causing the high frequency and low frequency regions to overlap (due to them being degenerate with each other). Two bandpass filters were separately used in conjunction with a 532 nm edge filter to collect both high/low frequency regions of the spectrum while avoiding aliasing issues caused by this overlap.

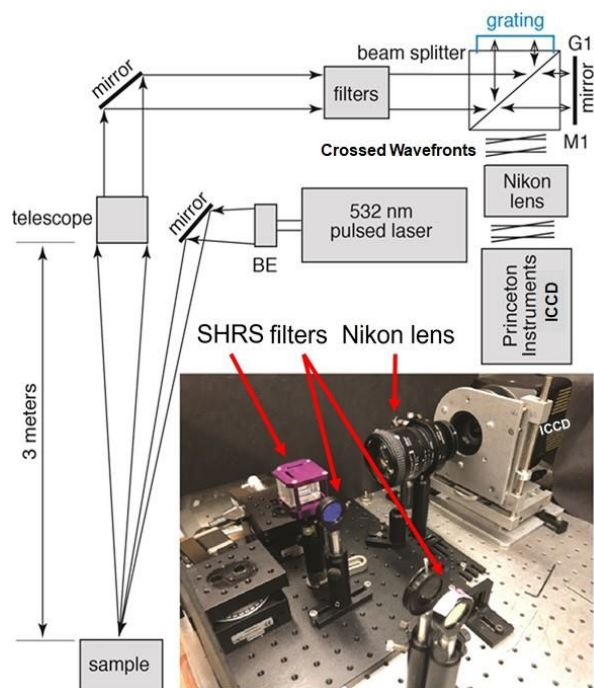


Figure 1: Contains the schematic diagram for the single grating (1g)-mSHRS setup along with an image of the 1g-mSHRS setup.

Results & Discussion: Figure 2 illustrates the time-resolved Raman spectra for both calcite and dolomite. Carbonates can have both biological and geological origins. This is especially true for calcite as its origin can be determined by Raman spectroscopy, depending on line widths and peak positions.[4] The most intense lines in both the CaCO_3 and $\text{CaMg}(\text{CO}_3)_2$ spectra are at 1085 and 1099 cm^{-1} , respectively. These correspond to the symmetrical stretching modes from the CO_3^{2-} ions and are fingerprints for these two minerals. The low frequency Raman shifts seen in the spectra are due to the external translational modes between the cation and anionic groups in the minerals, while the shifts between 700 and 750 cm^{-1} are due to deformation of the carbonate ions.[45,46] The low frequency translational lattice modes and high frequency stretching modes of CaCO_3 and $\text{CaMg}(\text{CO}_3)_2$ are at different positions from each other and allow for the unambiguous identification of both minerals.

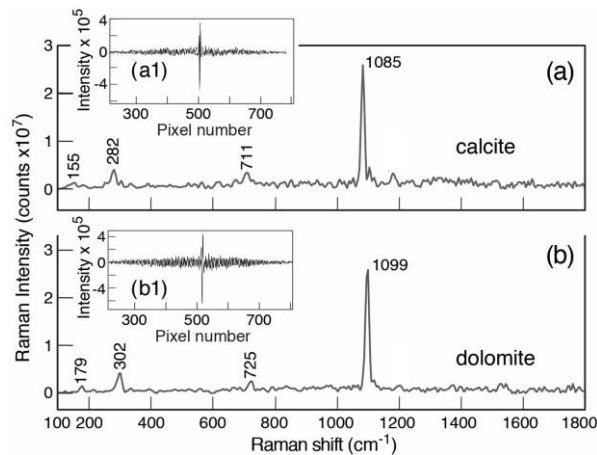


Figure 2: Raman spectra along with fringe image cross sections in the inserts of the carbonate minerals measured with the 1g-mSHRS at 3 m distance: calcite (CaCO_3) and dolomite ($\text{CaMg}(\text{CO}_3)_2$), as marked on the spectral traces. The setup used was 0.9x for both spectra with each spectrum only being 1 accumulation. The accumulation time for both the samples was 45s.

Table 1 compares the 1g-mSHRS instrumental properties to other SHRS instruments tested previously. The two-gratings mSHRS had two gratings, which gave it the highest resolving power and best theoretical MRF. This is despite the fact that the 1g-SHRS has a larger grating and, thus, more grooves per grating. The larger grating in the 1g-SHRS meant that the resolving power is larger than the 1g-mSHRS, even though both devices had the same number of gratings. The spectral range follows the opposite trend—it increases as the resolving power decreases. In addition, the mSHRS and 1g-SHRS were both used in the 2D SHRS configuration, which allows for an increase in the spectral range. The 2D configuration is achieved by apply a $1-2^\circ$ tilt along the optical axis.

Table 1: Contains the experimental values for the two-gratings monolithic SHRS (2g-mSHS), one-grating SHRS (1g-SHS), and single-grating monolith-SHRS (1g-mSHS) instrument for comparison. MRF stands for minimum resolvable feature.

| Instrument | Resolving Theoretical | | | Spectral Range | Grating Size | Groove Density |
|------------|-----------------------|---------------------------------|--------------------------|---|--------------|----------------|
| | Power (R) | Resolution (cm^{-1}) | MRF (cm^{-1}) | Exp/Theoretical Resolution (cm^{-1}) | (mm) | (l/mm) |
| 2g-mSHRS | 4752 | 3.9 | 9 | 2.31 | 3500 | 15 |
| 1g-SHRS | 3810 | 4.9 | 7.5 | 1.53 | 4915 | 25.4 |
| 1g-mSHRS | 2376 | 7.9 | 9 | 1.15 | 7327 | 15 |

One of the main benefits of the 1g-mSHRS over the 2g-mSHRS system is the addition of the mirror which increases the spectral range while lowering the resolving power. The reduction in resolving power is not a hindrance because one problem with the SHS system is the resolution is usually higher than is optimal. Additionally, the spectral range of the 1g-mSHRS could be doubled by employing the 2D SHRS configuration. This configuration, along with a camera with more pixels, would allow for the SHS system on a rover/helicopter (robotic explorer) to perform Raman, LIBS, UV, VIS, and IR spectroscopy all with one type of device.

Additionally, the monolith itself is $3.5 \times 3.5 \times 2.5$ cm and weighs 80g making it an interesting candidate for implementation on aerial vehicles, one to other planets. The success of the Ingenuity helicopter on the Mars 2020 Mission further expands on the utility of the SHS and shows potential for utilization on NASA's 2027 Dragonfly mission to Titan.[5]

Conclusions: This setup integrates the beam-splitter, grating, and mirror into a single monolithic device. This reduces the number of adjustable components, allows for easier alignment, and reduces the footprint of the device ($35 \times 35 \times 25$ mm with a weight of 80 g). This instrument provides a high spectral resolution ($\sim 9 \text{ cm}^{-1}$) and large spectral range (7327 cm^{-1}) while decreasing the sensitivity to alignment with a field of view of 5.61 mm at 3m. In conclusion, the 1g-mSHRS combines the benefits of both dispersive and FT Raman spectroscopy to create a robust, lightweight system with a small footprint, high resolution, high light throughput, high SNR, large spectral range, and with no moving parts making it a good candidate for planetary exploration

Acknowledgments: This work was supported by the University of South Carolina (USC) and University of Hawaii under a joint NASA PICASSO grant (#80NSSC19K1024). USC would like to thank the National Science Foundation (grant #OCE-18293330) for funding a part of this work. The authors would also like to thank Nancy Hulbirt and May Izumi for their valuable help with figures and editing.

References: [1] Wiens, R. C. et al. (2020) *Space Science Reviews*, 217 (1), 4. [2] Egan, M. J. (2020) *Journal of Raman Spectroscopy*, 51 (9), 1794-1801. [3] Waldron, A. (2020) *Applied Spectroscopy*, 75 (1), 57-69. [4] Zolotoyabko, E. et al. (2010) *Crystal Growth & Design*, 10 (3), 1207-1214. [5] Lorenz, R. D. et al. (2021) *The Planetary Science Journal*, 2 (1), 24.